

Effective Action Studies of Quantum Hall Spin Textures

K. Lejnell¹, A. Karlhede¹ and S. L. Sondhi².

¹ *Department of Physics, Stockholm University, Box 6730, S-11385 Stockholm, Sweden*

² *Department of Physics, Princeton University, Princeton NJ 08544*

(March 28, 2021)

We report on analytic and numerical studies of spin textures in quantum Hall systems using a long-wavelength effective action for the magnetic degrees of freedom derived previously. The majority of our results concern skyrmions or solitons of this action. We have constructed approximate analytic solutions for skyrmions of arbitrary topological and electric charge and derived expressions for their energies and charge and spin radii. We describe a combined shooting/relaxational technique for numerical determination of the skyrmion profiles and present results that compare favorably with the analytic treatment as well as with Hartree-Fock studies of these objects. In addition, we describe a treatment of textures at the edges of quantum Hall systems within this approach and provide details not reported previously.

73.40Hm

I. INTRODUCTION

Following the demonstration in [1] that quantum Hall ferromagnets contain skyrmions in their quasiparticle spectra, there has been a great deal of work on spin textures in quantum Hall systems. This work has received considerable impetus from a set of experiments [2–5] that have adduced evidence for skyrmions being the lowest energy quasiparticles at $\nu = 1$ as well as for their *not* being so at $\nu = 3$ and higher odd integer fillings [6,7]. The skyrmions themselves have been investigated by several authors [8,9] and a skyrme crystal phase has been studied [10] with a recent experiment appearing to find a transition into it at a finite temperature [11]. In addition, textured quasiparticles have been discussed in the context of double layer systems [12] and invoked in explaining a novel phase transition in the latter [13]. More recently, it has been shown that ferromagnetic quantum Hall states can exhibit textured edges [14,15].

The analysis in [1] was based on a long wavelength effective action for the spin dynamics, supplemented by a charge density-topological density constraint, that allowed an analytic computation of the properties of the skyrmions in the limit of small Zeeman energies. No details of this computation were given there and one of the purposes of this paper is to provide them. A second is to report numerical studies of the effective action, that have a region of validity beyond the analytic approximations, and compare extremely well with those using the Hartree-Fock technique of Fertig *et. al.* [8]. We also

report here on the details of effective action studies of the textured edges mentioned in [14]. We note that the numerical studies have been described previously in a thesis by one of us [16] and are being reported here for ease of access. In the interim, effective action results on skyrmion properties have been reported by Abolfath *et. al.* using methods similar to ours [17], and by Rao *et. al.* using a variational approach [18], while Moon and Mullen have presented an improved action that is accurate even for small skyrmion sizes [19].

The paper is organized as follows. After introducing the effective action in Sec. II, we outline the analytic derivation of skyrmion properties at small Zeeman energies in Sec. III. In Sec. IV, we discuss the technique utilized in their numerical computation. In Sec. V, we present the numerical results for charge 1 and charge 2 skyrmions at $\nu = 1$, and compare to Hartree-Fock calculations and analytic expansions. We then discuss the asymptotic shape of the skyrmions (Sec. VI). This is followed by results for textured edges (Sec. VII) and a brief summary (Sec. VIII).

II. EFFECTIVE ACTION AND SKYRMIONS

In the long wavelength limit, the spin degree of freedom of a quantum Hall (QH) ferromagnet is described by a unit vector $\mathbf{n}(\mathbf{r})$. A distinguishing feature of QH ferromagnets is that the topological density of the spin field, $q(\mathbf{r}) = \mathbf{n} \cdot (\partial_x \mathbf{n} \times \partial_y \mathbf{n})/4\pi$, is proportional to the deviation of the charge density, $\rho(\mathbf{r})$, from its background value, $\rho - \bar{\rho} = \nu_{FM} q$ where $\bar{\rho} = \nu_{FM}/2\pi\ell^2$. (ν_{FM} is the filling factor of the ferromagnetic component of the QH liquid (*e.g.* $\nu_{FM} = 1$ at $\nu = 3$), and $\ell = \sqrt{\hbar c/eB}$ is the magnetic length.) This enables one to formally integrate out the dynamics of the charge and obtain an effective Lagrangian for the system in terms of the spin field alone whose coefficients can be fixed using known long wavelength quantities [1]:

$$\mathcal{L}_{eff} = \frac{1}{2} \bar{\rho} \mathcal{A}(\mathbf{n}) \partial_t \mathbf{n} - \frac{1}{2} \rho_s (\nabla \mathbf{n})^2 + \frac{1}{2} g \bar{\rho} \mu_B \mathbf{n} \mathbf{B} - \nu_{FM}^2 \frac{e^2}{2\epsilon} \int d^2 r' \frac{q(\mathbf{r}) q(\mathbf{r}')}{|\mathbf{r} - \mathbf{r}'|} . \quad (1)$$

Here, \mathcal{A} is the vector potential of a unit magnetic monopole, ρ_s is the spin stiffness [20] and ϵ the dielectric constant of the background semiconductor. Technically, \mathcal{L}_{eff} describes an $O(3)$ σ -model.

As we will be interested in this paper in static configurations of the field, we will seek to minimize the energy functional

$$E = - \int d^2r [\mathcal{L}_{eff} - \frac{1}{2} \bar{\rho} \mathcal{A}(\mathbf{n}) \partial_t \mathbf{n}] \equiv E_G + E_Z + E_C \quad , \quad (2)$$

where the gradient (E_G), the Zeeman (E_Z) and the Coulomb (E_C) energies can be read off from Eq. (1). In the following we will measure all energies in units of $e^2/\epsilon\ell$ and lengths in units of ℓ .

For finite energy configurations, the finiteness of the gradient term requires that the field approach a common value at infinity regardless of direction. In such cases, the plane can be compactified to a sphere and $\mathbf{n}(\mathbf{r})$ gives a map from S_2 (the compactified plane) to S_2 (spin space or the target space of the σ -model). Such maps are characterized by an integer topological charge Z , which can be expressed as $Z = \int d^2r q(\mathbf{r})$, where q is the topological (Pontryagin) density introduced earlier. As noted there, the topological density plays a crucial role in the physics of QH ferromagnets as it is proportional to the charge density of the underlying itinerant system. Consequently, localized configurations of topological charge Z , which we shall term charge Z skyrmions, carry electric charge $\nu_{FM} Z |e|$.

In the absence of the Zeeman and Coulomb terms, the energy functional (2) is scale invariant and rotationally invariant but on account of the non-linearity implicit in the definition of \mathbf{n} , finding its skyrmion solutions is a non-trivial problem, solved previously by Belavin and Polyakov (BP) [21,22]. The additional terms break both symmetries although they preserve rotations about the field axis which we shall take to be the z -axis. For the full action, the BP technique (based on achieving a Bogomol'nyi bound [23] for the action) breaks down with the non-locality of the Coulomb term making matters even worse. Consequently, it is necessary to attack the Euler-Lagrange equation for the energy functional directly.

We now derive this equation for the skyrmion configurations by making an ansatz that has topological charge Z and depends on one unknown function. Calculating the energy of this configuration and minimizing with respect to the unknown function gives an integro-differential equation.

In the ground state the spin of the ferromagnetic component is polarized: $\mathbf{n} = \hat{z}$. For a skyrmion with topological charge Z , we make the ansatz (in polar coordinates (r, θ) with their origin at the center of the skyrmion):

$$\begin{aligned} n_x &= \sqrt{1 - f^2(r)} \cos(Z\theta) \quad , \\ n_y &= \sqrt{1 - f^2(r)} \sin(Z\theta) \quad , \\ n_z &= f(r) \quad . \end{aligned} \quad (3)$$

This leads to the topological density

$$q(\mathbf{r}) = \frac{Z}{4\pi r} \frac{df}{dr} \quad . \quad (4)$$

For a finite energy configuration, the spin vector must be aligned with the external magnetic field at infinity. At the center the spin points in the opposite direction. This leads to the boundary conditions $f(0) = -1$, $f(\infty) = 1$, and (4) shows that (3) describes configurations with topological charge Z . Note that the topological density is independent of θ , *i.e.* it is spatially rotationally invariant; since a shift $\theta \rightarrow \theta - \theta_0$ in (3) is a spin rotation it is clear that the topological density is invariant under spin rotations about the z -axis as well. Note however, that the spin field itself is not separately invariant under rotations and spin rotations — it is invariant only under the combination generated by $L_z + ZS_z$. It is easy to convince oneself that respecting both symmetries is incompatible with non-trivial skyrmion solutions. Consequently, our ansatz is the maximally symmetric one possible. Examples of spin configurations for $Z = 1$ and $Z = 2$ are sketched in Fig. 1.

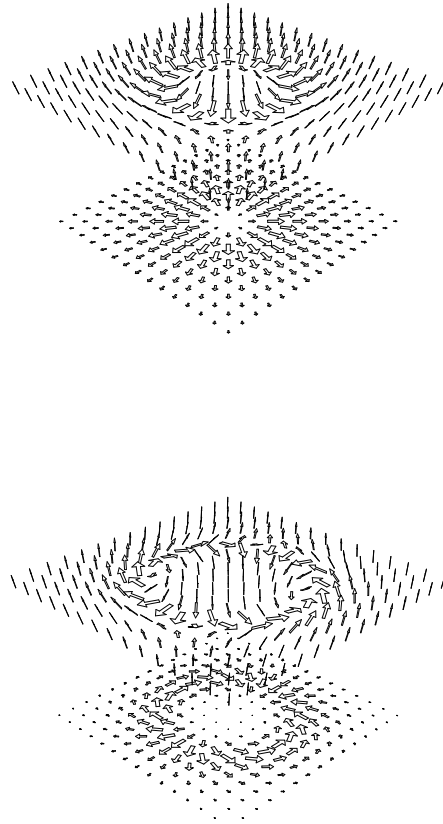


FIG. 1. Skyrmion spin vector field, $\mathbf{n}(\mathbf{r})$, and its projection onto the plane of the electron gas for $Z = 1$ (top figure) and $Z = 2$ (bottom figure).

The function $f(r)$ in (3) is determined by minimizing the energy (2). We now calculate the energy for a skyrmion of the form (3). The gradient and Zeeman energies are:

$$E_G = \pi\rho_s \int_0^\infty dr \left[Z^2 \frac{1-f^2}{r} + \frac{rf'^2}{1-f^2} \right] , \quad (5)$$

$$E_Z = -\frac{1}{2}\nu_{FM}\tilde{g} \int_0^\infty dr r f(r) , \quad (6)$$

where $\tilde{g} = g\mu_B B / (e^2/\epsilon\ell)$ and $f' = df/dr$. We write the Coulomb energy as

$$E_C = \frac{1}{4}\nu_{FM}^2 Z^2 \int_0^\infty dr f' V_C(r, f') , \quad (7)$$

where

$$V_C(r, f') = \frac{1}{4\pi} \int_0^\infty dr' f'(r') \int_0^{2\pi} d\theta' [r^2 + r'^2 - 2rr' \cos(\theta' - \theta)]^{-1/2} \\ = \frac{1}{\pi} \int_0^\infty dr' \frac{f'(r')}{r+r'} \cdot F\left(\frac{\pi}{2}, 2\frac{\sqrt{rr'}}{r+r'}\right) . \quad (8)$$

Here, $F(\varphi, x)$ is the elliptic integral of the first kind [24].

Adding all energy contributions, (5), (6) and (7), we obtain the final expression for the total energy:

$$E = \int_0^\infty dr \left[\pi\rho_s \left(Z^2 \frac{1-f^2}{r} + \frac{rf'^2}{1-f^2} \right) - \frac{1}{2}\nu_{FM}\tilde{g}rf + \frac{1}{4}\nu_{FM}^2 Z^2 f' V_C(r, f') \right] . \quad (9)$$

Varying the energy functional with respect to f we find (observing that $\delta E_C / \delta f$ gives a contribution $-2\partial V_C / \partial r$) the non-linear and non-local integro-differential equation:

$$[r^2 f'' + r f'](1-f^2) + r^2 f f'^2 + [Z^2 f + \frac{\tilde{g}\nu_{FM}}{4\pi\rho_s} r^2 + \frac{\nu_{FM}^2 Z^2}{4\pi\rho_s} r \frac{\partial V_C}{\partial r}] \cdot (1-f^2)^2 = 0 . \quad (10)$$

Note that V_C is a functional of f .

As we noted earlier, the gradient energy, E_G , is scale invariant and that minimizing it alone leads to the BP solutions of arbitrary size λ . Rewriting Eq. (5) as

$$E_G = \mp 4\pi\rho_s Z + \pi\rho_s \int_0^\infty dr \frac{r}{1-f^2} \left[f' \pm \frac{Z(1-f^2)}{r} \right]^2 , \quad (11)$$

we find the Bogomol'nyi bound on the energy

$$E_G[f] \geq 4\pi\rho_s |Z| , \quad (12)$$

and solving $rf' \pm Z(1-f^2) = 0$ we obtain the BP solutions,

$$f(r) = \frac{(r/\lambda)^{2|Z|} - 4}{(r/\lambda)^{2|Z|} + 4} , \quad (13)$$

with energy $E_G = 4\pi\rho_s |Z|$.

The energy E is independent of the sign of Z , hence each solution $f(r)$ to (10) describes both a skyrmion ($Z > 0$) and an antiskyrmion ($Z < 0$). In the following, when we talk about skyrmions, and assume Z is positive, the results are equally valid for antiskyrmions with negative charge provided we replace Z by $|Z|$.

By contrast to the BP solutions, the skyrmions in the QH ferromagnet have a definite size set by a competition between the Coulomb energy, E_C , and the Zeeman energy, E_Z . The Coulomb energy favors large skyrmions since it decreases when charge is spread out. The Zeeman energy, on the other hand, increases when more spins are flipped, *i.e.* when the skyrmion becomes larger, and thus favors small skyrmions. This leads to a competition that determines an optimal size and energy of the skyrmion.

In the next section we will construct approximate analytic solutions to Eq. (10) and in sections IV and V we will describe numerical solutions obtained by a relaxation procedure.

III. ANALYTIC TREATMENT

We begin by recalling the Bogomol'nyi bound (12) on the gradient energy of a configuration with topological charge Z , $E_G[f] \geq 4\pi\rho_s Z$. The Coulomb self-interaction of a charge distribution is non-negative, $E_C \geq 0$, and upon dropping a negative extensive constant which implies that we are measuring excitation energies relative to the ferromagnetic ground state configuration, $E_Z \geq 0$ as well. Consequently, $E[f] \geq 4\pi\rho_s Z$.

We will be interested in large skyrmions, for which the long-wavelength effective action approach will be accurate. As remarked previously, this will be the case when E_C ‘‘dominates’’ E_Z , *i.e.* as $\tilde{g} \rightarrow 0$. In this limit of divergent skyrmion size, it is clear that $E_C \ll 1$ whence by a general balance argument the *value* of $E_Z \sim E_C \ll 1$ as well. Consequently, as $\tilde{g} \rightarrow 0$, the energy of the skyrmion will approach the Bogomol'nyi bound and we expect that the solution itself will converge to a BP solution with an appropriately chosen λ .

It turns out that this observation is sufficient to determine the leading small \tilde{g} characteristics of the skyrmions with $Z \geq 2$, but needs to be supplemented by global considerations for $Z = 1$. These follow from identifying the various length scales in the problem by pairwise balancing the terms, $E_G \sim 1$, $E_C \sim 1/\lambda$ and $E_Z \sim \tilde{g}\lambda^2$, in the energy functional. This yields three scales: $R_1 \sim 1$ (E_G and E_C), $R_2 \sim 1/\tilde{g}^{1/3}$ (E_Z and E_C) and $R_3 \sim 1/\tilde{g}^{1/2}$ (E_Z and E_G). Note that *two* of these scales diverge as $\tilde{g} \rightarrow 0$ with $R_3 \gg R_2$. Hence a global solution to (12) in this limit can be expected to exhibit *both* of these scales.

We have not succeeded in constructing such a global solution, which appears to be a difficult task due to the non-locality of the equation. Instead we will attempt to formally perturb around the BP solutions. To lowest order, this is a problem in degenerate perturbation theory and requires merely that we minimize $E_G + E_Z + E_C$ in the subspace of the BP solutions. By construction, E_G is a constant in this subspace. The relevant integral for the Zeeman term can be done analytically, and yields,

$$E_Z = \nu_{FM} \pi \frac{2^{2/Z-1} \csc(\pi/Z)}{Z} \tilde{g} \lambda^2 \quad . \quad (14)$$

For $Z = 1$, the double integral for the Coulomb term can be carried out as well:

$$E_C = \nu_{FM}^2 \frac{3\pi^2}{128} \frac{1}{\lambda} \quad (Z = 1) \quad . \quad (15)$$

However, for $Z \geq 2$ we had to take recourse to numerical integration with the results,

$$\begin{aligned} E_C &= \nu_{FM}^2 \frac{1.49}{\lambda} \quad (Z = 2) \\ &= \nu_{FM}^2 \frac{4.16}{\lambda} \quad (Z = 3) \\ &= \nu_{FM}^2 \frac{8.41}{\lambda} \quad (Z = 4) \quad . \end{aligned} \quad (16)$$

Note that E_Z ($Z = 1$) is infinite. Putting this aside for the moment, we minimize $E_Z + E_C$ with respect to λ for $Z \geq 2$ to find,

$$\begin{aligned} \lambda &= 0.780(\nu_{FM}/\tilde{g})^{1/3} \text{ and} \\ E &= 2 \left[\sqrt{\frac{\pi}{32}} + 1.43(\nu_{FM}^5 \tilde{g})^{1/3} \right] \quad (Z = 2) \\ \lambda &= 1.29(\nu_{FM}/\tilde{g})^{1/3} \text{ and} \\ E &= 3 \left[\sqrt{\frac{\pi}{32}} + 1.61(\nu_{FM}^5 \tilde{g})^{1/3} \right] \quad (Z = 3) \\ \lambda &= 1.75(\nu_{FM}/\tilde{g})^{1/3} \text{ and} \\ E &= 4 \left[\sqrt{\frac{\pi}{32}} + 1.80(\nu_{FM}^5 \tilde{g})^{1/3} \right] \quad (Z = 4) \quad . \end{aligned} \quad (17)$$

We will see later on that these provide an excellent description of the numerically determined solutions at small \tilde{g} , as expected.

The physically interesting case of $Z = 1$ is more difficult. One can see from Eq. (13) that $1 - f(r) \sim 1/r$ at large r , whence E_Z diverges logarithmically with system size. Consequently, the BP solutions *cannot* be used to globally approximate the true solutions at any value of $\tilde{g} \neq 0$; the latter must exhibit a faster decay of $1 - f(r)$ at large r .

The asymptotic behavior of the true solutions can be obtained directly from the equation of motion (10). At points far from the core, the Zeeman term in the equation dominates over the Coulomb term. The latter is

the potential of a localized charge distribution and will decay asymptotically as $1/r$. Dropping the latter, setting $f = 1 - \psi^2/2$ and linearizing shows that ψ satisfies Bessel's equation,

$$r^2 \psi'' + r \psi' - (Z^2 + \frac{\nu_{FM} \tilde{g} r^2}{4\pi \rho_s}) \psi = 0 \quad (18)$$

with the physical solution ($\psi \rightarrow 0$ as $r \rightarrow \infty$) $\psi \propto K_Z(r/R_3)$ in terms of the scale $R_3 = \sqrt{\frac{4\pi \rho_s}{\nu_{FM} \tilde{g}}}$ introduced earlier. As $K_Z(x) \sim \sqrt{\frac{\pi}{2x}} e^{-x}$ for $x \gg 1$, the true asymptotic behavior of $1 - f$ is exponential for *all* Z , different from the corresponding BP solutions.

For $Z \geq 2$, this discrepancy will (presumably) be attenuated by going to higher orders in the expansion about the BP solutions - but it has no bearing on the validity of the leading small \tilde{g} behavior derived previously. For $Z = 1$, we will make the *assumption* that matching an inner BP solution to an outer exponentially decaying solution (the minimal fix for the divergence encountered) will yield the leading small \tilde{g} behavior. (Such a solution will certainly converge pointwise to a BP solution, but we have not shown that the corrections to it are subdominant. For $Z \geq 2$ one can readily show that this is the case by linearizing about the optimized BP solution [25].) More precisely, we assume that,

$$\begin{aligned} f(r) &= \frac{(r/\lambda)^2 - 4}{(r/\lambda)^2 + 4} \quad , \quad r \ll R_3 \\ &= 1 - \frac{a_1^2}{2} K_1^2\left(\frac{r}{R_3}\right) \quad , \quad r \gg \lambda \end{aligned} \quad (19)$$

is the desired solution at small \tilde{g} (for $Z = 1$: $a_1^2 = 16\lambda^2/R_3^2$). It is easy to check that with this choice of a , both pieces of the definition of f agree on the interval $\lambda \ll r \ll R_3$ where they overlap.

Assuming $\lambda \ll R_3$, we find that, with the above choice of f ,

$$E_Z = 4\nu_{FM} \tilde{g} \lambda^2 \ln\left(\frac{R_3}{a_1 \lambda}\right) \quad , \quad (20)$$

where $\ln(a_1) = \frac{1}{2} + \gamma$, *i.e.* $a_1 = 2.9365$. Combining this with our earlier expression for E_C , we are required to minimize

$$E(\lambda) = \frac{\beta}{\lambda} + \alpha \tilde{g} \lambda^2 \ln\left(\frac{1}{\lambda} \sqrt{\frac{\delta}{\tilde{g}}}\right) \quad (21)$$

with $\alpha = 4\nu_{FM}$, $\beta = \frac{3\pi^2 \nu_{FM}^2}{128}$ and $\delta = 4\pi \rho_s / a_1^2 \nu_{FM}$ in the region $\lambda \ll R_3$, *i.e.* $\lambda \sqrt{\tilde{g}} \ll 1$. Differentiating with respect to λ and setting $\lambda^3 = (3\beta/2\alpha)\lambda^3$ then leads to the transcendental equation,

$$\frac{1}{\lambda^3} = \tilde{g} \ln\left(\frac{c}{\lambda^3 \tilde{g}^{3/2}}\right) \quad (22)$$

with $c = (2\alpha/3\beta)(\delta/e)^{3/2}$. As c involves ρ_s , which depends on ν , it does not scale trivially with ν ; for $\nu = 1$ it equals 0.0178. Eq. (22) has solutions only for \tilde{g} below some critical value, \tilde{g}_{c3} . For $\nu = 1$, one finds $\tilde{g}_{c3} = 4.3 \times 10^{-5}$. At this point $\lambda = 12.6$, hence the condition $\lambda\sqrt{\tilde{g}} \ll 1$ is obeyed and we also note that $c/\sqrt{\tilde{g}_{c3}} = 2.7$.

Equation (22) can be solved perturbatively at small \tilde{g} by replacing λ^3 in the argument of the logarithm by the full RHS. This yields, to second order in this procedure,

$$\frac{1}{\lambda^3} = \frac{2\alpha}{3\beta} \tilde{g} \{ \ln(c/\sqrt{\tilde{g}}) + \ln \ln(c/\sqrt{\tilde{g}}) + O(\ln \ln(c/\sqrt{\tilde{g}})/\ln(c/\sqrt{\tilde{g}})) \} \quad (23)$$

for the parameter λ and thereafter

$$E(\tilde{g}) = \sqrt{\frac{\pi}{32}} + A[\tilde{g} \ln(c/\sqrt{\tilde{g}})]^{1/3} \left\{ 1 + \frac{1}{3} \frac{\ln \ln(c/\sqrt{\tilde{g}})}{\ln(c/\sqrt{\tilde{g}})} + \frac{1}{2} \frac{1}{\ln(c/\sqrt{\tilde{g}})} + O((\ln \ln(c/\sqrt{\tilde{g}})/\ln(c/\sqrt{\tilde{g}}))^2) \right\} \quad (24)$$

(with $A = 3 * (\alpha/3)^{1/3} (\beta/2)^{2/3} = 0.7838$) for the energy of the skyrmion. In all of these expressions, the scale for \tilde{g} is set by $c^2 \approx 3 * 10^{-4}$ which is quite small. This comes about as the argument of the logarithm is essentially the ratio R_3/R_2 and the asymptotic regime starts to make sense only when this ratio is $O(1)$. As this ratio grows extremely weakly, as $\tilde{g}^{1/6}$, one has to go to fairly small \tilde{g} before entering asymptopia and as a result the scale of the logarithms, which is set by the scale of this crossover, is small. We also note, as discussed at more length elsewhere, that the logarithmic enhancement of the energies of the $Z = 1$ skyrmions relative to their $Z = 2$ cousins causes them to bind at extremely small values of \tilde{g} [26].

Finally, we can use the leading solutions developed here to compute various measures of the size of the skyrmions. Quantities of particular interest are the spin of the skyrmions and their root mean squared spin and charge radii defined via:

$$\begin{aligned} S_z &= \bar{\rho} \int d^2r \frac{1}{2} (1 - f(r)) \\ R_s^2 &= \langle r^2 \rangle_s \equiv \bar{\rho} \int d^2r r^2 \frac{1}{2} (1 - f(r)) / S_z \\ R_c^2 &= \langle r^2 \rangle_c \equiv \frac{1}{Z} \int d^2r r^2 q(r) \quad , \end{aligned} \quad (25)$$

where we have approximated the local density of electrons, $\rho(r) = \bar{\rho} + \nu_{FM} q(r)$, by $\bar{\rho} = \nu_{FM}/2\pi$. These quantities are not all independent; an integration by parts shows that $S_z = \nu_{FM} R_c^2/2$, and, moreover, since $E_Z = \tilde{g} S_z$, the spin is obtained from (14) and (20).

For the spin radius we find,

$$R_s = \sqrt{\frac{2}{3}} \frac{R_3}{\ln^{1/2}(\frac{R_3}{a_1 \lambda})} \quad (Z = 1)$$

$$\begin{aligned} &= 2\sqrt{\frac{2}{\pi}} \lambda \ln^{1/2}\left(\frac{R_3}{a_2 \lambda}\right) \quad (Z = 2) \\ &= (2^{2/Z-1} \sec(\pi/Z))^{1/2} \lambda \quad (Z \geq 3) \end{aligned} \quad (26)$$

with $\ln(a_2) = \gamma - \frac{1}{12} - \frac{\ln 2}{2}$. Note the feature, that depending on the charge of the skyrmion and the highest power of radius in the integrand, we get different scales entering the leading dependence.

IV. NUMERICAL METHODS

Here we describe how we numerically solve Eq. (10). We use mainly a relaxation technique [27], however, due to numerical problems at $r = 0$ for $\tilde{g} > 10^{-3}$, we must combine this with a shooting method in order to achieve high numerical precision [28]. We begin by describing the relaxation method.

A. Relaxation technique

The idea of the relaxation method is to start from an ansatz, f , for a solution to the differential equation (DE), $\mathbf{D}(f) = 0$, and then use a first order Taylor expansion to improve this ansatz iteratively. We want to find Δf so that $\mathbf{D}(f + \Delta f) = 0$; expanding to first order we have

$$\mathbf{D}(f) + \int dr \frac{\delta \mathbf{D}}{\delta f} \cdot \Delta f = 0 \quad . \quad (27)$$

Solving for Δf gives the improved function $f + \Delta f$. To implement this on a computer, we first rewrite the N^{th} order differential equation as N coupled first order equations (in our case $N = 2$). We then put the system on a lattice and replace the differential equations by finite difference equations (FDE). The resulting algebraic equations relate the values of the functions $\mathbf{f} = (f^1, f^2, \dots, f^N)$ (where $f^1 = f, f^2 = df/dr \dots$) at lattice points k (\mathbf{f}_k) and $k + 1$ (\mathbf{f}_{k+1}):

$$\mathbf{D}_k(r_k, r_{k+1}, \mathbf{f}_k, \mathbf{f}_{k+1}) = 0 \quad , \quad (28)$$

here \mathbf{D}_k are the FDEs at lattice point k . Taylor expanding as in (27) gives

$$\begin{aligned} \mathbf{D}_k(\mathbf{f}_k + \Delta \mathbf{f}_k, \mathbf{f}_{k+1} + \Delta \mathbf{f}_{k+1}) &\approx \mathbf{D}_k(\mathbf{f}_k, \mathbf{f}_{k+1}) \\ + \sum_{\alpha=1}^N \frac{\partial \mathbf{D}_k}{\partial f_k^\alpha} \Delta f_k^\alpha + \sum_{\alpha=1}^N \frac{\partial \mathbf{D}_k}{\partial f_{k+1}^\alpha} \Delta f_{k+1}^\alpha &= 0 \quad . \end{aligned} \quad (29)$$

These equations are then solved for the increments $\Delta \mathbf{f}_k$ and the procedure is iterated until the corrections, $\Delta \mathbf{f}_k$, are small enough. As a measure of the error we use:

$$err = \frac{1}{M \cdot N} \sum_{k=1}^M \sum_{\alpha=1}^N |\Delta f_k^\alpha| \quad , \quad (30)$$

where M is the number of lattice points [29]. If the error is large only a fraction of the correction is used when calculating the new function, this reduces the risk for over-correction near $f = \pm 1$ where the DE is very sensitive to disturbances in f . After each iteration we calculate the energy, using equation (9), and check that it decreases.

B. Numerical solution for small \tilde{g}

There are two problems to solve before we can apply the relaxation method: First, the boundary conditions are given at $r = 0$ and at $r = \infty$ but we can only cover a finite interval $[0, r_{max}]$ with the M lattice points (with the DE in the above form). This is a problem for large skyrmions, *i.e.* when \tilde{g} is small. Second, the relaxation method relies on the validity of a first order Taylor expansion, therefore it is crucial to make an ansatz that is close to the true solution.

To minimize the finite size effects we solve the equations for several different r_{max} and extrapolate to infinite system size. Fig. 2 shows how the energy scales with $1/r_{max}$ for $\tilde{g} = 5 \cdot 10^{-4}$ and $5 \cdot 10^{-6}$. We see that the energy is more or less independent of system size at the largest sizes, whence the finite size effects are negligible. The spin, and the spin radius, show bigger finite size effects and scaling to infinite system size is necessary to obtain accurate values when $\tilde{g} \lesssim 10^{-6}$.

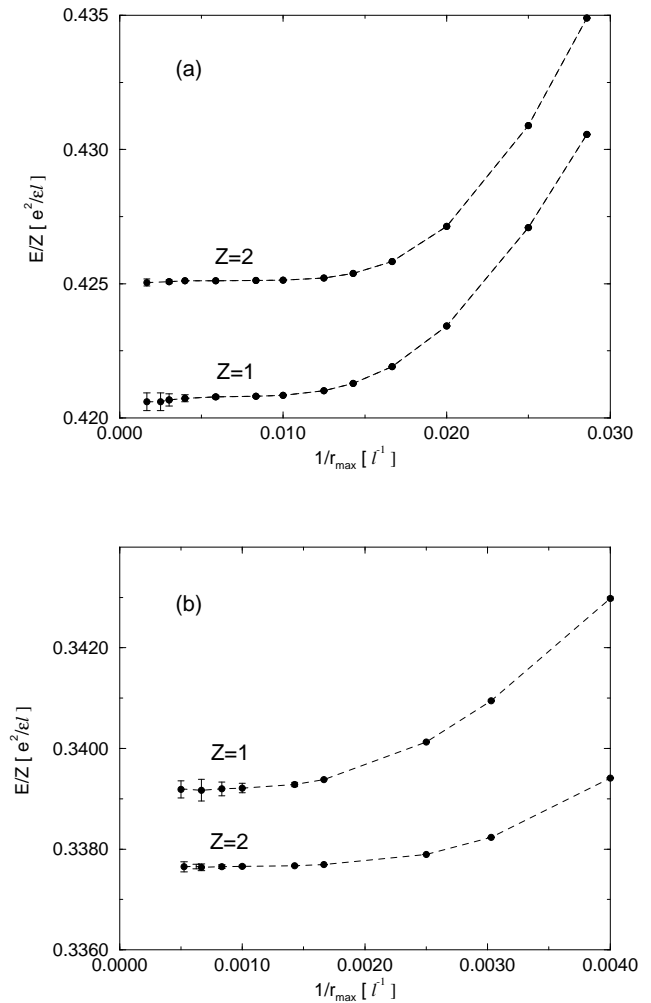


FIG. 2. Skyrmion energies (per charge Z) as functions of system size for (a) $\tilde{g} = 5 \cdot 10^{-4}$ and (b) $\tilde{g} = 5 \cdot 10^{-6}$, at $\nu = 1$.

To obtain a good initial ansatz is a bit tricky; we proceed as follows. The Belavin-Polyakov solution, Eq. (13), to the scale invariant model is expected to be a good approximation to the true solution in the core region (for some value of the scale parameter λ), see Sec. III. As our ansatz we therefore use this solution with the function $const \cdot r^Z$ added, where we choose the constant so that the boundary condition $f(r_{max}) = 1$ is fulfilled. We run the relaxation procedure for different λ and choose the one for which the convergence is best.

Having determined an ansatz we can start iterating. The Coulomb term $V_C(r, f')$, which enters the DE, depends on the integral over f' . Thus we start each iteration by calculating the function $V_C(r, f')$ using the most recent f . Then we iterate until the error is small enough, each time checking that the energy decreases.

To check the accuracy of the solution we use a shooting test. The relaxation solution is used as input to the shooting method (fourth order Runge-Kutta). We pick a

point r_0 close to $r = 0$ (e.g. the first lattice point where $f' \neq 0$) and treat the problem as an initial value problem with $f(r_0)$ and $f'(r_0)$ given from the relaxation solution. If the shooting solution thus obtained coincides with the relaxation solution we are confident that this is the right solution. Comparing the energy obtained from the relaxation and the shooting solutions we find, for both $Z = 1$ and $Z = 2$, that for the smallest \tilde{g} ($\tilde{g} \approx 10^{-7}$) this difference is of the order of 10^{-5} . The difference is approximately constant up to $\tilde{g} = 10^{-4} - 10^{-3}$. For $\tilde{g} \gtrsim 10^{-3}$ the difference starts to grow; this is also reflected in the convergence properties of the relaxation method. This indicates that the ansatz we use deviates more from the true solution and the relaxation method has problems avoiding the singular behavior near $r = 0$.

C. Larger \tilde{g}

The problems for larger \tilde{g} ($\tilde{g} \gtrsim 10^{-3}$) has to do with the structure of the differential equation (10) at the origin together with a smaller overlap between the solution and the ansatz. In this region we proceed as follows. The solution obtained from an initial set of relaxation iterations is used to shoot from the point r_0 [28] (close to $r = 0$) to a point a finite distance away from $r = 0$. This point is then used as a boundary point for a set of new relaxation iterations. With this method, which is illustrated in Fig. 3, we avoid the problems near $r = 0$ [30].

This method certainly introduces an error in the calculation. As a rough estimate of the error we take the energy difference between the initial relaxation solution and the solution obtained by the combined relaxation and shooting method. For $\tilde{g} = 0.02$ this is of the order of one percent. (Hartree-Fock theory [8] shows that the skyrmion has a size of a few magnetic lengths and consists of a few flipped spins at $\tilde{g} = 0.02$. Whereas Hartree-Fock should be correct in this region, the validity of the effective long-distance theory becomes questionable at distances of the order of the magnetic length.) For a comparison between Hartree-Fock and effective action results see Sec. V below.

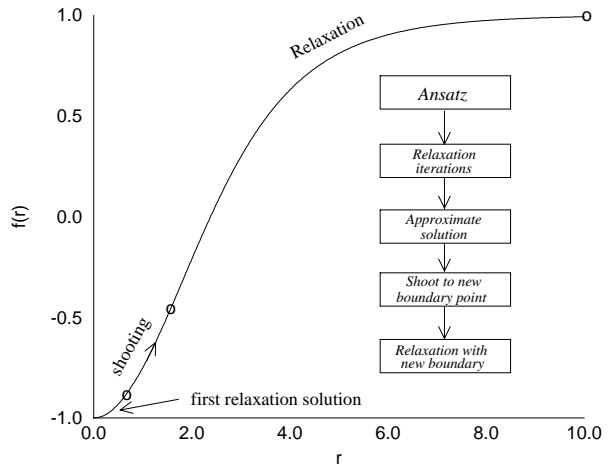


FIG. 3. Sketch of the numerical method used to solve the equations of motion for $\tilde{g} > 10^{-3}$.

V. NUMERICAL RESULTS

We have applied the technique described in Sec. IV to skyrmions with topological charge $Z = 1, 2$ and 3 at $\nu = 1$, i.e. $\nu_{FM} = 1$, $\rho_s = 1/16\sqrt{2\pi}$. Our results are presented in Figs. 4-9. The $Z = 3$ skyrmion is not found to be the lowest energy excitation for any \tilde{g} considered here (in agreement with the analytic result, Sec. III), we therefore show results for $Z = 1$ and $Z = 2$ skyrmions only.

Fig. 4 shows the z -component of the spin, $n_z = f$, as a function of the radius, r . An analysis shows that for $Z = 2$ at $\tilde{g} = 5 \cdot 10^{-4}$, the numerical solution agrees very well in the core region with the Belavin-Polyakov solution (13), with λ determined by Eq. (17). For $Z = 1$, no analytic solution is available for the values of \tilde{g} shown in the figure, however for $\tilde{g} < \tilde{g}_{c3} = 4.3 \cdot 10^{-5}$, the numerical solution agrees well with the analytic solution (13), with λ determined by Eq. (23). Away from the core region, the relaxation solutions differ from the BP solutions, although the differences are quite small for $Z = 2$.

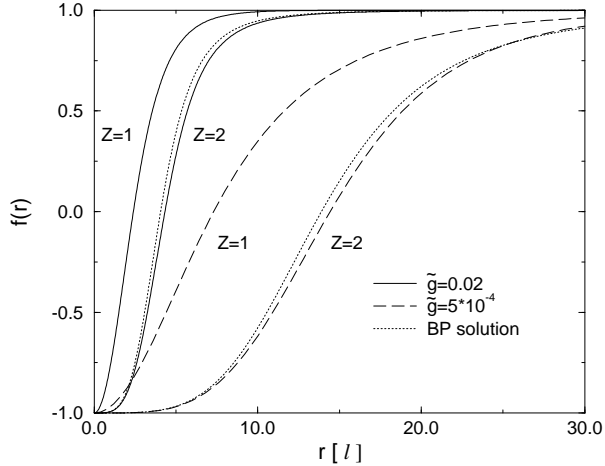


FIG. 4. The relaxation solution, $f(r)$, for $\tilde{g} = 0.02, 0.0005$ and $Z = 1, 2$. $Z = 2$ is compared to the Belavin-Polyakov solution (13), with the scale, λ , taken from Eq. (17).

From the numerical solution $f(r)$ we calculate the energy of the skyrmion using Eq. (9). In Fig. 5, the energy of the $Z = 1, 2$ skyrmions, relative to the groundstate energy $E_{(f=1)} = -\frac{1}{4}\tilde{g}r_{max}^2$, is given as a function of \tilde{g} and compared to Hartree-Fock (HF) results [8,31]. We see that the effective and Hartree-Fock theories agree very well for small \tilde{g} , but that the HF energy is substantially lower for larger values of \tilde{g} . In particular, the effective theory predicts that the skyrmions are the lowest energy charged excitations for $\tilde{g} < 0.018$ whereas HF gives $\tilde{g} < \tilde{g}_{c1} = 0.054$. The difference between effective action and Hartree-Fock results is smaller for $Z = 2$ than for $Z = 1$.

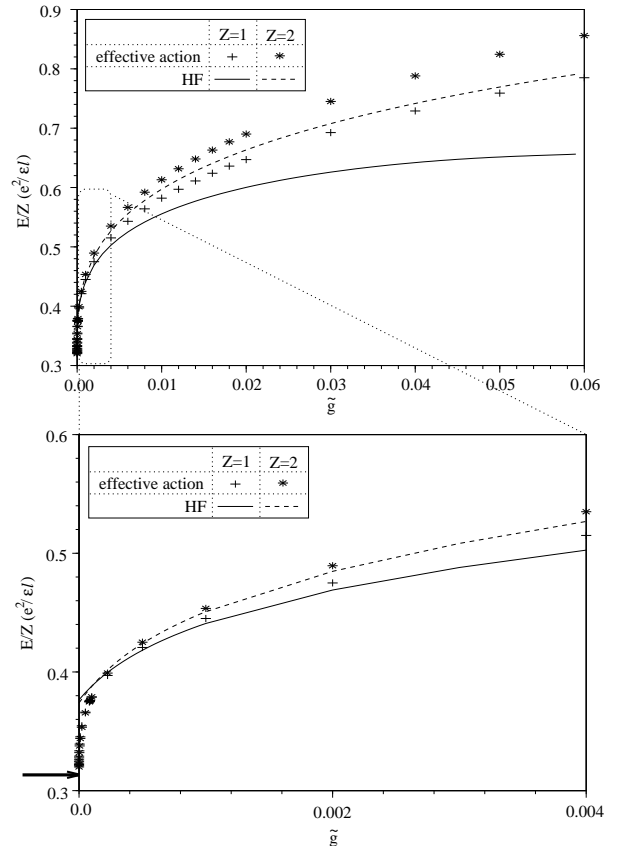


FIG. 5. Effective action and Hartree-Fock results for the energy, E , per charge (relative to the ground state) of the $Z = 1, 2$ skyrmions as function of \tilde{g} . (Due to finite size effects in the HF calculation the HF energy becomes larger than the effective action energy for very small \tilde{g} .) The arrow in the inset marks the energy at $\tilde{g} = 0$.

The effective theory is a long distance theory valid only for large smooth skyrmions, *i.e.* for small enough \tilde{g} . Hartree-Fock theory, on the other hand, is valid all the way from polarized quasiparticles and very small skyrmions near $\tilde{g}_{c1} = 0.054$ to quite large skyrmions (where finite size effects eventually limit the applicability of HF). It is interesting to note that the effective theory works quite well also for fairly large values of \tilde{g} . In the limit of very small \tilde{g} , the effective theory becomes exact (see Sec. III) and E/Z approaches $\sqrt{\pi/32}$ (marked by \rightarrow in the figure). The blowup in Fig. 5 shows a region (close to $\tilde{g} = 0$) where the Hartree-Fock energy is larger than the effective action energy, this is an effect of the difficulty of handling large enough systems in Hartree-Fock. Since in this range, the skyrmions become very large (see Fig. 8) finite size effects make the Hartree-Fock energies unreliable. For $\tilde{g} < \tilde{g}_{c2} = 8.4 \times 10^{-5}$, the $Z = 2$ skyrmions actually have lower energy (per charge) than the $Z = 1$ skyrmions, *i.e.* the $Z = 1$ skyrmions bind in pairs [26].

We now compare the analytic small \tilde{g} expansions for the energy, derived in Sec. III, with the numerical effective action results. Fig. 6 shows the skyrmion energies for $10^{-7} \lesssim \tilde{g} \lesssim 10^{-6}$; the inset shows the $Z = 2$ energies for larger \tilde{g} . For $Z = 2$ the agreement is excellent all the way up to $\tilde{g} = 0.06$. For $Z = 1$, the numerical results are seen to approach the analytic result Eq. (24) as $\tilde{g} \rightarrow 0$, however, deviations are still visible at $\tilde{g} = 10^{-7}$. The size of these is consistent with the size of the ignored correction terms in Eq. (24). Note that the correction terms decrease extremely slowly with decreasing \tilde{g} .

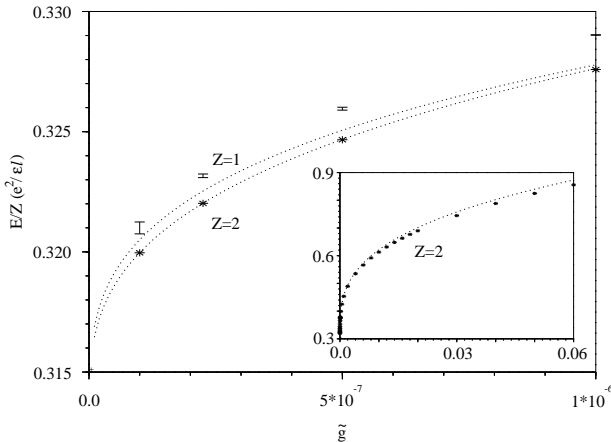


FIG. 6. Numerical effective action results (points) for the energy compared with the analytic expressions, Eq. (24) and (17), (lines) for $Z = 1, 2$ skyrmions. The error bars come from finite size effects, for $Z = 2$ the error bars are smaller than the dots. The inset shows the $Z = 2$ data for large \tilde{g} .

Fig. 7 shows the spin, S_z , of the $Z = 1, 2$ skyrmions relative to the groundstate, see Eq. (25). Since $S_z = R_c^2/2$ this also gives the (topological) charge radius, R_c . The numerical effective action results and the Hartree-Fock results become indistinguishable, for $Z = 1$ as well as for $Z = 2$, as \tilde{g} approaches zero but, in fact, agree quite well over the whole range although deviations are observable for larger \tilde{g} . The analytic small \tilde{g} expansions agree extremely well with the numerical effective action results for all \tilde{g} for $Z = 2$ and for $\tilde{g} < \tilde{g}_{c3}$ for $Z = 1$.

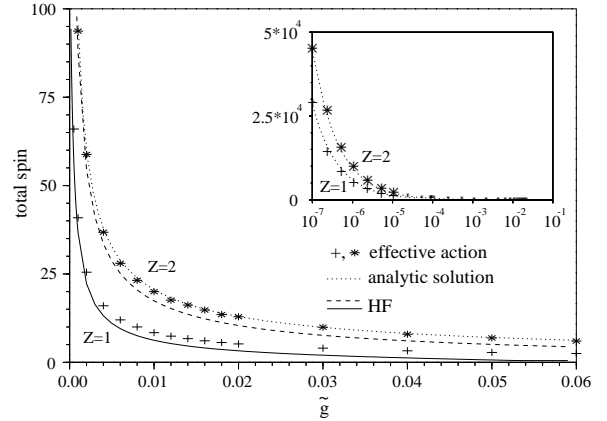


FIG. 7. Spin, S_z , for $Z = 1, 2$ skyrmions; numerical effective action results compared to HF and analytic small \tilde{g} expansions. The inset shows results for very small \tilde{g} where no HF data are available. For $Z = 1$, the analytic expansion breaks down at $\tilde{g}_{c3} = 4.3 \times 10^{-5}$.

Fig. 8 shows how the spin radii, R_s , see Eq. (25), of the skyrmions decrease with increasing \tilde{g} . The $Z = 2$ spin radius is smaller than the $Z = 1$ radius for $\tilde{g} \lesssim 10^{-3}$.

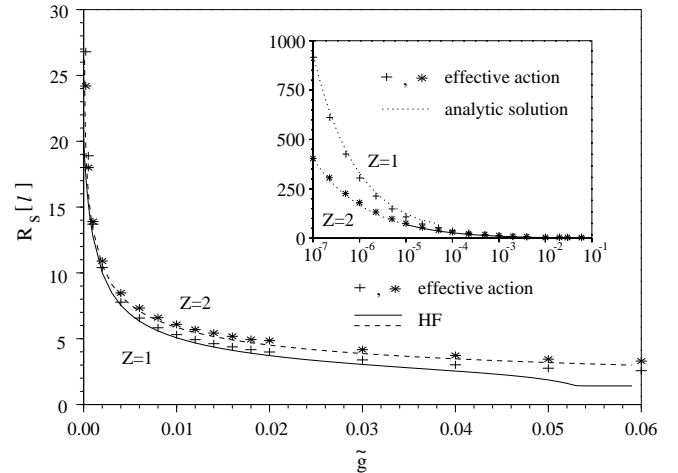


FIG. 8. Spin radii for $Z = 1, 2$ skyrmions; numerical effective action results compared to HF and analytic small \tilde{g} expansions. The spin radii for $Z = 1$ and $Z = 2$ are equal at $\tilde{g} \sim 10^{-3}$.

In Fig. 9 we show spin and charge density profiles. A comparison between the Hartree-Fock and effective action densities reveals almost identical profiles at $\tilde{g} = 5 \cdot 10^{-4}$, see [32], whereas at $\tilde{g} = 0.02$ the profiles deviate substantially. We also note that the agreement for the $Z = 2$ skyrmion is better than the agreement for the $Z = 1$ skyrmion (at large \tilde{g}).

$$1 - f(r) \propto \frac{R_3}{r} e^{-2r/R_3} . \quad (31)$$

The crossover to this regime can be estimated by examining the behavior of the Bessel functions for *small* values of their argument:

$$K_Z(x) \sim \frac{2^{Z-1}\Gamma(Z)}{x^Z} , \quad (32)$$

which shows that the crossover sets in at $x^Z \sim 2^{Z-1}\Gamma(Z)$, for example, at $r \sim R_3$ ($Z = 1$) and $r \sim \sqrt{2}R_3$ ($Z = 2$), *i.e.* farther out for higher Z . To compare these observations with the numerical solution we plot $\ln[r(1 - f(r))]$ against r for $Z = 1$ and $Z = 2$, at $\nu = 1$, see Fig. 10. When $\tilde{g} = 5 \cdot 10^{-6}$, $R_3 = 250$ and we get a straight line for $r > 400$ when $Z = 1$ and for $r > 700$ when $Z = 2$; in qualitative agreement with our above observation. Reading off the slope for $Z = 1$ in the figure and comparing to Eq. (31) one finds $R_3 = 247 \pm 9$, in excellent agreement with the exact value $R_3 = 250$. For $Z = 2$, the exponential region sets in further out and, in addition, the curve bends up slightly for $r > 1000$ due to finite size effects in combination with the finite resolution of real numbers in the computer, therefore this curve is harder to analyze. However, comparing the curve for several different system sizes and keeping the part which is unchanged, one finds that it is consistent with an exponential behavior with $R_3 = 250$.

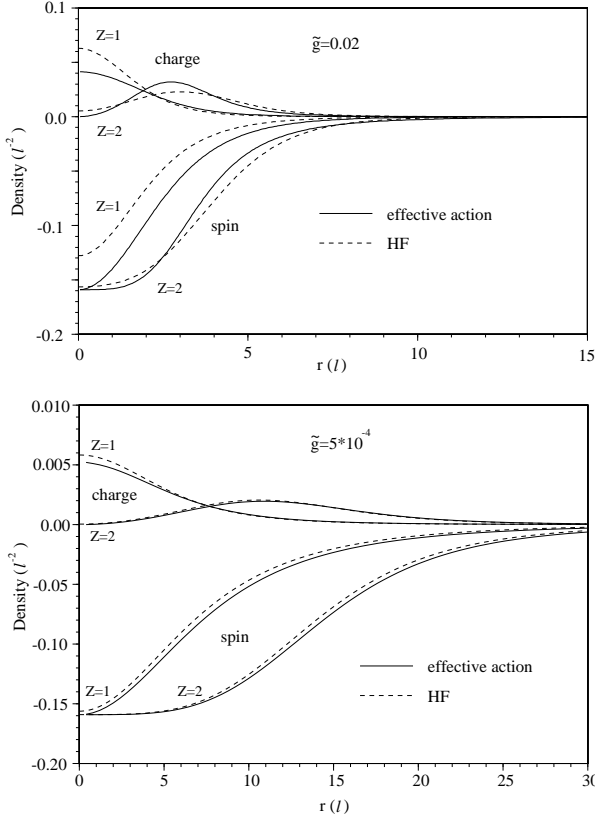


FIG. 9. Spin and charge density profiles for $Z = 1, 2$ skyrmions; effective action and HF results.

VI. ASYMPTOTIC SHAPE OF THE SKYRMION

Here we will examine the detailed profile of the skyrmions in two regions, near the center and far from the center, where it is possible to compute it rigorously. This serves as a further check on our analysis.

A. Small r

Since the charge distribution is radially symmetric it is clear that $\partial V_C / \partial r|_{r=0} = 0$. This implies that both the Zeeman and the Coulomb terms in the differential equation (10) can be neglected and the solution is given by the Belavin-Polyakov solution, Eq. (13). This is consistent with the numerical solutions, see Fig. 4.

B. Large r

As we showed in Sec. III, far from the core, $r \gg R_3$, the skyrmion profile, $1 - f(r) \propto K_Z^2(r/R_3)$, is exponential,

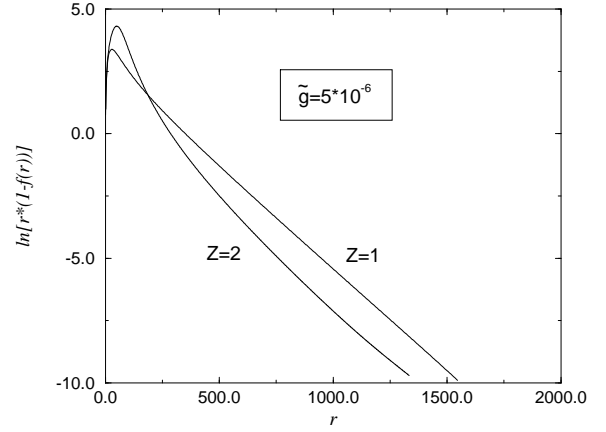


FIG. 10. Numerical effective action result for the asymptotic behavior of $f(r)$, at $\nu = 1$. Both the $Z = 1$ and the $Z = 2$ cases are well described by the asymptotic formula derived in the text.

VII. EDGES

In previous work [14] we have used the effective theory to study the reconstruction of a sharp polarized edge of a semi-infinite quantum Hall ferromagnet as the confining

potential is softened. The problem of reconstruction is as follows. For hard confinement, the ferromagnetic bulk state continues all the way out to the edge and the density drops abruptly to zero over the scale of the magnetic length. When the edge potential softens, charge eventually moves out, *i.e.* the edge reconstructs. The question is how this happens given the competition between the correlation energy of the quantum Hall state and the Hartree energy due to the confinement. In [14] we argued that the initial instability, as the potential softens, is to forming a spin texture along the edge [15]. Charge is then moved out as a consequence of the spin-charge relation of spin textures. Here we will give details, previously unpublished, of how the formation of edge textures is analyzed within the effective theory. (Before proceeding, the following caveat is in order. The use of an unmodified magnetic action near the edge is not unproblematic given that there are gapless density modes near the edge among other things. While we have not attempted to derive an action for the edge from microscopics, we have checked [14] by comparison with Hartree-Fock calculations, that the action we use is accurate for getting static properties of the edge at small \tilde{g} .)

We consider a semi-infinite Hall system occupying the region $x < 0$ (y is the direction along the edge). As an ansatz for the spin vector field $\mathbf{n}(\mathbf{r})$ we take

$$\begin{aligned} n_x &= \sqrt{1 - f^2(x)} \cos(ky) , \\ n_y &= \sqrt{1 - f^2(x)} \sin(ky) , \\ n_z &= f(x) . \end{aligned} \quad (33)$$

This leads to the topological density

$$q(x) = \frac{k}{4\pi} f'(x) , \quad (34)$$

where $f'(x) = df/dx$. The z -component of the spin, $f(x)$, gradually falls from one in the bulk, to some value f_e ($-1 \leq f_e \leq 1$) at the edge. As one moves along the edge the spin in the xy -plane rotates with wave number k . f_e and k are continuous parameters that are to be determined. Note that, although locally this texture is identical to the texture for bulk skyrmions there is no quantization: $\int d^2r q(\mathbf{r})$ can take any value.

The electron density, $\rho(x)$, is

$$\begin{aligned} \rho &= \bar{\rho} + \nu_{FM} q(x) , & -\infty < x \leq x_R \\ \rho &= 0 , & x_R < x . \end{aligned} \quad (35)$$

The unreconstructed, sharp polarized edge corresponds to taking $f(x) = 1$, $x \leq 0$ and $f(x) = 0$, $0 < x$. This case is obtained by letting $q(x) = 0$, $x_R = 0$ in (35). When the edge is textured, charge is moved out and x_R is determined by charge conservation: $\int_{-\infty}^{x_R} dx \rho = \int_{-\infty}^0 dx \bar{\rho}$. This gives,

$$x_R = \frac{k}{2} (1 - f_e) . \quad (36)$$

We assume the confining potential is caused by a positively charged background density, $\rho_b(x)$, that falls linearly from its bulk value, $\bar{\rho} = \nu_{FM}/2\pi$, to zero over a region of width w centered around $x = 0$. The strength of the confining potential is varied by varying the parameter w . For small w the sharp polarized edge is favored, but as w increases the edge will reconstruct.

For a spin texture of the form (33) one finds the following gradient, Zeeman and Coulomb energy densities (per unit length of the edge):

$$\begin{aligned} E_G &= \frac{\rho_s}{2} \int_{x_L}^{x_R} dx [k^2(1 - f^2) + \frac{f'^2}{1 - f^2}] , \\ E_Z &= \frac{\nu_{FM} \tilde{g}}{4\pi} \left[\frac{k}{4} (1 - f_e^2) - \int_{x_L}^{x_R} dx f \right] , \\ E_C &= -\nu_{FM}^2 \int_{x_L}^{w/2} \int_{x_L}^{w/2} dx dx' \delta\rho(x) \delta\rho(x') \ln|x - x'| . \end{aligned} \quad (37)$$

Here, x_L is chosen such that $f(x) = 1$ for $x \leq x_L$, and $\delta\rho(x) = \rho(x) - \rho_b(x)$ is the deviation of the electron density from the background density.

Varying the total energy $E = E_G + E_Z + E_C$ with respect to f , we find

$$\begin{aligned} f''(1 - f^2) + f f'^2 \\ + [k^2 f + \frac{\tilde{g} \nu_{FM}}{4\pi \rho_s} + \frac{\nu_{FM}^2 k}{\rho_s} \partial V_C / \partial x] (1 - f^2)^2 = 0 \quad , \end{aligned} \quad (38)$$

where

$$\begin{aligned} V_C(x, f') &= \int_{x_L}^{x_R} \frac{dx'}{2\pi} [\rho_b(x') - \bar{\rho} - \frac{k}{4\pi} f'(x')] \ln|x - x'| \\ &+ \int_{x_R}^{w/2} \frac{dx'}{2\pi} \rho_b(x') \ln|x - x'| . \end{aligned} \quad (39)$$

We solve Eq. (38) using the relaxation method described in Sec. IV. As an initial ansatz for f , we take a modified BP solution $f_{BP}(x) = (x^2 - 4\lambda^2)/(x^2 + 4\lambda^2)$ (*c.f.* Eq. (13)) that obeys the boundary conditions $f(x_L) = 1$, $f(x_R) = f_e$:

$$f_{ans}(x) = f_e + (1 - f_e) \frac{1 + f_{BP}(x_R - x)}{1 + f_{BP}(x_R - x_L)} . \quad (40)$$

The ansatz depends on one parameter λ (for given f_e). In the numerical procedure we vary this parameter until we get convergence.

We can now study whether a spin textured edge has lower energy than the sharp polarized edge for given parameters (\tilde{g}, w) . In particular, we can determine the phase transition line in the (\tilde{g}, w) -plane where the sharp edge reconstructs by forming a spin textured edge. Solving Eq. (38) using the relaxation method for given boundary condition f_e and wave number k determines $f(x)$. The energy of this state is calculated from Eq.

(37) and k is determined by minimizing this energy. This gives the energy of the state $E(\tilde{g}, w, f_e)$. $f_e = 1$ gives the energy for the sharp edge. We find that the spin textured edge is lower in energy than the sharp edge for any f_e if and only if the derivative of the energy at $f_e = 1$ is positive: $\partial E(\tilde{g}, w, f_e)/\partial f_e|_{f_e=1} > 0$. The result is that the textured edge has lower energy in a triangular region of parameter space, for small \tilde{g} and big enough w , see [14].

VIII. SUMMARY

We have used a long wavelength magnetic effective action to compute various properties of quantum Hall skyrmions and find that these compare favorably with those obtained by more microscopic Hartree-Fock calculations and by analytic small \tilde{g} expansions. We have also used the effective action to reliably predict the onset of texturing at the edges of quantum Hall ferromagnets for small values of the Zeeman energies. Taken together, these show that this formalism and the relaxational technique presented here have great utility in the study of quantum Hall ferromagnets.

ACKNOWLEDGMENTS

We are grateful to Steven Kivelson for useful discussions and to Daniel Lilliehöök for providing Hartree-Fock results. This work was supported in part by NSF grant No. DMR-96-32690, the A. P. Sloan Foundation and the Institute for Advanced Study (SLS), and the Swedish Natural Science Research Council (AK).

[1] S. L. Sondhi, A. Karlhede, S. A. Kivelson and E. H. Rezayi, Phys. Rev. B **47**, 16419 (1993). See also, E. H. Rezayi, Phys. Rev. B **36**, 5454 (1987) and **43**, 5944 (1991); D.-H. Lee and C. L. Kane, Phys. Rev. Lett. **64**, 1313 (1990).

[2] S. E. Barrett, G. Dabbagh, L. N. Pfeiffer, K. W. West and R. Tycko, Phys. Rev. Lett. **74**, 5112 (1995). See also, R. Tycko, S. E. Barrett, G. Dabbagh, L. N. Pfeiffer and K. W. West, Science **268**, 1460 (1995).

[3] A. Schmeller, J. P. Eisenstein, L. N. Pfeiffer and K. W. West, Phys. Rev. Lett. **75**, 4290 (1995).

[4] E. H. Aifer, B. B. Goldberg and D. A. Broido, Phys. Rev. Lett. **76**, 680 (1996).

[5] D. K. Maude *et. al.*, Phys. Rev. Lett. **77**, 4604 (1996).

[6] X. G. Wu and S. L. Sondhi, Phys. Rev. B **51**, 14725 (1995).

[7] J. K. Jain and X. G. Wu, Phys. Rev. B **49**, 5085 (1994).

[8] H. A. Fertig, L. Brey, R. Côté and A. H. MacDonald, Phys. Rev. B **50**, 11018 (1994); H. A. Fertig *et. al.*, Phys. Rev. B **55**, 10671 (1997).

[9] There is by now a sizable literature on this subject and we apologize for not listing much of the recent work except where directly germane to the topic of this paper.

[10] C. Timm, S. M. Girvin and H. A. Fertig, “Skyrmion lattice melting in the quantum Hall system”, preprint, cond-mat/9804057 and references therein.

[11] V. Bayot, E. Grivei, S. Melinte, M. B. Santos, M. Shayegan, Phys. Rev. Lett. **76**, 5484 (1996).

[12] K. Yang, K. Moon, L. Zheng, A. H. MacDonald, S. M. Girvin, D. Yoshioka and S.-C. Zhang, Phys. Rev. Lett. **72**, 732 (1994); K. Moon, H. Mori, K. Yang, S. M. Girvin, A. H. MacDonald, L. Zheng, D. Yoshioka and S.-C. Zhang, Phys. Rev. B **51**, 5138 (1995).

[13] S. Q. Murphy, J. P. Eisenstein, G. S. Boebinger, L. N. Pfeiffer and K. W. West, Phys. Rev. Lett. **72**, 728 (1994).

[14] A. Karlhede, S. A. Kivelson, K. Lejnell and S. L. Sondhi, Phys. Rev. Lett. **77**, 2061 (1996).

[15] For related work see, B. E. Kane, L. N. Pfeiffer and K. W. West, Phys. Rev. B **46**, 7264 (1992); J. H. Oaknin, L. Martin-Moreno, C. Tejedor, Phys. Rev. B **54**, 16850 (1996); M. Franco and L. Brey, Phys. Rev. B **56**, 10383 (1997); A. Karlhede and K. Lejnell, Physica E1, 42 (1997); J. M. Leinaas and S. Viefers, Nucl. Phys. B **520**, 675 (1998).

[16] K. Lejnell, “A Long Wavelength Study of Quantum Hall Skyrmions”, Thesis (Stockholm University, 1996).

[17] M. Abolfath, J. J. Palacios, H. A. Fertig, S. M. Girvin and A. H. MacDonald, Phys. Rev. B **56**, 6795 (1997).

[18] M. Rao, S. Sengupta and R. Shankar, Physica E1, 54 (1997).

[19] Kyungsun Moon and Kieran Mullen, “An accurate effective action for ‘baby’ to ‘adult’ skyrmions, preprint, cond-mat/9707250.

[20] For $\nu = 3, 1, 1/3$ and $1/5$ $\rho_s/(e^2/\epsilon\ell)$ equals 4.36×10^{-2} , 2.49×10^{-2} , 9.23×10^{-4} and 2.34×10^{-4} respectively.

[21] A. A. Belavin and A. M. Polyakov, Pis'ma ZhETF **22**, 503 (1975) [Soviet Physics JETP Letters **22**, 245 (1975)].

[22] For a review see R. Rajaraman, *Solitons and Instantons* (North-Holland, Amsterdam, 1982).

[23] E. B. Bogomol'nyi, Sov. J. Nucl. Phys. **24**, 449 (1976).

[24] See, *e.g.* I. S. Gradshteyn and I. M. Ryzhik, *Table of Integrals, Series, and Products* (Academic Press, New York, 1980).

[25] Ar. Abanov and V. L. Pokrovsky, “Skyrmion in a real magnetic film”, preprint, cond-mat/9801114.

[26] D. Lilliehöök, K. Lejnell, A. Karlhede and S. L. Sondhi, Phys. Rev. B **56**, 6805 (1997).

[27] W. H. Press, S. A. Teukolsky, W. T. Vetterling, and B. P. Flannery, *Numerical Recipes in C* (Cambridge University Press, 1988).

[28] The shooting method cannot be used directly since the origin is a critical point: The value of the function and of its first derivative at the origin do not specify the solution uniquely.

[29] To be precise, we give different weights to the errors in the function and in the derivative; this is because their typical values differ.

- [30] An alternative method would be to use the sigma model solution near $r = 0$. We would then have to minimize the energy with respect to additional parameters (corresponding to unknown derivatives of f at the origin) and this would necessarily involve several relaxation solutions. This is quite time consuming and also has other numerical disadvantages.
- [31] We give the energies to create one skyrmion at fixed particle number and fixed magnetic field. These energies are equal for the skyrmion and antiskyrmion (with the same value of $|Z|$).
- [32] The deviation is probably partly due to finite size effects in the Hartree-Fock calculation for which the boundary condition is $f(r_{max}) = 1$ at $r_{max} \approx 32\ell$ while in the effective action calculation we have $r_{max} = 600\ell$.